JOURNAL OF SOLID STATE CHEMISTRY 120, 64–69 (1995)

XRD and Mössbauer Studies on Oxygen-Deficient Ni(II)-Bearing Ferrite with a High Reactivity for CO_2 Decomposition to Carbon

T. Kodama,[1] M. Tabata, T. Sano, M. Tsuji, and Y. Tamaura

Department of Chemistry, Research Center for Carbon Recycling & Utilization, Tokyo Institute of Technology, 2-12-1, Ookayama, Meguro-ku, Tokyo 152, Japan

Received March 30, 1995; in revised form June 19, 1995; accepted June 21, 1995

CO_2 decomposition to carbon at 300°C was studied using H_2-reduced Ni(II)-bearing ferrite. The oxygen-deficient Ni(II)-bearing ferrite (ODNF: $Ni_{0.39}Fe_{2.61}O_{4-\delta}$) was formed by H_2-reduction of $Ni_{0.39}Fe_{2.61}O_4$ (NF) at 300°C. The ODNF was characterized by X-ray diffractometry and Mössbauer spectroscopy before and after CO_2 decomposition. The oxygen deficiency (δ) of ODNF increased with an increase in an H_2-reduction time. It decreased after CO_2 decomposition. The reactivity of ODNF for CO_2 decomposition increased with a higher δ value. The lattice constant of the ODNF was larger than that of the stoichiometric NF, which decreased, approaching the stoichiometric value after CO_2 decomposition. Mössbauer spectra suggest that excess iron ions in interstices of octahedral sites migrate to tetrahedral sites in a spinel structure of the ferrite by incorporating oxygens from CO_2 during CO_2 decomposition.

INTRODUCTION

Spinel ferrite, $M_xFe_{3-x}O_4$, generally exhibits nonstoichiometry due to excess oxygen (1–5). The lattice constant of the ferrite unit cell decreases with an increase in oxygen, indicating the presence of vacant cation sites (1, 3). Recently, the present authors and co-workers reported that oxygen-deficient or cation-excess ferrite (ODF) is formed as a metastable phase during the H_2 reduction of spinel ferrite at 300°C (6–10). The ODF can be represented by the chemical formula $M_xFe_{3-x}O_{4-\delta}$ (M = Fe, Zn, and Mn): the oxygen deficiency δ expresses the degree of reduction. The lattice constant increases with an increase in the oxygen deficiency δ, which will be due to changes in cation dimension and repulsion associated with reduction of Fe^{3+} to Fe^{2+} in the ferrite. The maximum value of δ in the $M_xFe_{3-x}O_{4-\delta}$ system is strongly dependent on the kind of divalent metal M: δ = 0.06 for Zn(II)-bearing ferrite and 0.15 for Mn(II)-bearing ferrite. The ODF is reduced directly to the component metals or the wüstite phase by a further H_2 reduction at 300°C, depending on the kind of ferrite (6–13).

The ODFs are highly reactive to CO_2, causing the decomposition of CO_2 to carbon and oxygen at 300°C (6–11). We have studied the decomposition of CO_2 over oxygen-deficient magnetite in the temperature range 150–300°C and found that the adsorption can be expressed by the Langumuir dissociative isotherm for three fragments: carbon and two oxygens (11). The carbon is deposited on the material surface and the oxygens are incorporated into the crystal lattice of the ferrite. The chemical form of the deposited carbon varies depending on the carbon density (C-density) on the material surface (14–16). At a low C-density, active atomic carbon is formed, which is easily converted to CH_4 by H_2 at 300°C. The atomic carbon is transformed to polymerized carbon at a high C-density which is less reactive to methanation.

In more recent research, Ni(II)-bearing ferrite reduced with H_2 at 300°C is found to show a much higher reactivity toward CO_2 decomposition in comparison with other divalent-metal ferrites (M = Fe, Zn, Mn, and Co) reduced with H_2 under similar conditions (17, 18). In the present paper, XRD and Mössbauer studies on oxygen-deficient Ni(II)-bearing ferrite (ODNF) with a high reactivity for CO_2 decomposition were performed.

EXPERIMENTAL

1. Preparation and Characterization of Ni(II)-Bearing Ferrite

Ni(II)-bearing ferrite (NF; $Ni_{0.39}Fe_{2.61}O_4$) was synthesized by the wet method according to the procedure reported previously (19–21). The product was identified by X-ray diffractometry with Cu$K\alpha$ radiation (Rigaku model RINT-2000 diffractometer). The Mössbauer spectra were recorded at room temperature with a ^{57}Co source diffused in metallic rhodium which was oscillated in a constant acceleration mode. The Doppler velocity scale was cali-

[1] Present address: Department of Chemistry & Chemical Engineering, Faculty of Engineering, Niigata University, 8050, Ikarashi 2-nocho, Niigata 950-21, Japan.

0022-4596/95 $12.00

brated with thin absorbers of α-Fe foil. The spectra were analyzed by a computer curve fitting method assuming pure Lorentzian line shapes. The chemical compositions were determined both by inductivity coupled plasma (ICP) spectroscopy (Seiko Instruments, model SPS7000) and by colorimetry (HITACHI, model U-1100) using 2,2′-dipyridyl (22) after dissolving the samples in an HCl solution. The lattice constants were calculated by the extrapolation ($\theta \rightarrow 90°$) of the linear Nelson–Riley function, $\cos^2\theta/\sin\theta + \cos^2\theta/\theta$, vs the lattice constant plot using the least-squares method (standard deviation $\sigma < 0.00002$) (23). From transmission electron microscopy (TEM), the crystallite size of the prepared NF was estimated to range from 50 to 200 nm. The BET surface area was 9.5 $m^2\ g^{-1}$.

2. CO_2 Decomposition with H_2-Reduced Ni(II)-Bearing Ferrite in a Batch System

CO_2 decomposition with H_2-reduced NF was performed in a batch mode as follows. A 1.0 g portion of the prepared NF was placed in the quartz tube of a reaction cell (8 mm i.d. × 300 mm length). H_2 gas was passed through the reaction cell (an H_2 flow rate = 18 $cm^3\ min^{-1}$) at 300°C for 30 or 60 min. After evacuating the reaction cell, 10 cm^3 of CO_2 gas was injected into the closed reaction cell. The pressure was measured with a pressure gauge, and the inner gas species were determined by gas chromatography (Shimadzu GC-8A). The sample before and after CO_2 decomposition was quenched by quickly placing the reaction cell into a refrigerant of ice–NaCl while passing nitrogen gas through and was identified by X-ray diffractometry and Mössbauer spectroscopy while protected from air oxidation. The carbon content of the samples was determined using an elemental analyzer (Perkin–Elmer, model 2400 CHN).

RESULTS AND DISCUSSION

1. CO_2-Decomposition with H_2-Reduced NF

Figure 1 shows the time variations of the partial pressures of CO_2 and CO in the reaction cell during CO_2 decomposition. The injected CO_2 gas was decomposed to carbon with H_2-reduced NF and the partial pressure of CO_2 gradually decreased. Very small amounts of CO were evolved during CO_2 decomposition. No other gases except for CO_2 and CO were detected in the reaction cell. The internal pressure decreased corresponding to the decrease in the partial pressure of CO_2. A black fine powder of carbon remained after dissolving the samples in an HCl solution after CO_2 decomposition. Concerning the mass balance of carbon, the amount of the diminution of CO_2 volume in the gas phase was nearly equivalent to the carbon content of the samples after CO_2 decomposition as estimated from elemental analysis (90% of the diminished CO_2). These results indicate that CO_2 gas was decomposed to carbon. The CO_2 decomposition attained 20 and 39% of the amount of injected CO_2 by volume in the NFs H_2-reduced for 30 and 60 min, respectively. The reactivity of the H_2-reduced NF for CO_2 decomposition increased with an increase in reduction time. For the NF reduced for 30 min, the partial pressures of CO_2 and CO became constant after 40 min of the reaction time. The CO_2 decomposition reaction attains equilibrium in approximately 60 min. For the NF reduced for 60 min, equilibrium was not attained in 60 min.

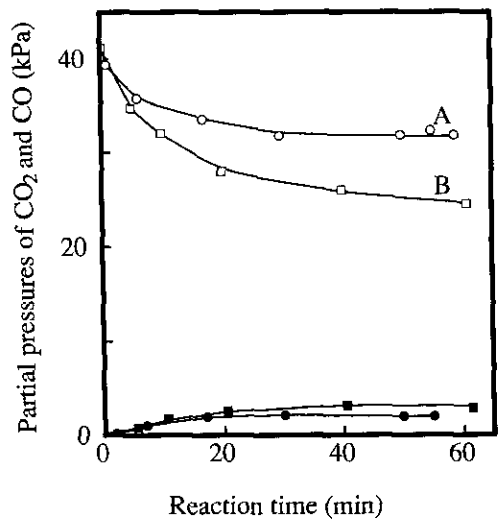

FIG. 1. Time variations of partial pressures of CO_2 and CO during CO_2 decomposition with H_2-reduced Ni(II)-bearing ferrite (NF). Open symbols are for CO_2 and solid symbols for CO. Circles are for the NF H_2 reduced for 30 min and squares for 60 min.

2. XRD Study on H_2-Reduced NF in CO_2 Decomposition

The XRD pattern corroborated that the prepared NF was a single-phase spinel structure (Fig. 2a). No peaks indicating the products NiO, $Ni(OH)_2$, α-Fe_2O_3, and iron oxide hydroxides such as α-FeO(OH) could be observed. The chemical compositions of the prepared NF and ODNF were determined as follows. Assuming that the sample is a single phase of a spinel compound which consists of Ni^{II}, Fe^{II}, Fe^{III}, and O^{2-}, x, y, z, and δ in the chemical formula $Ni^{II}_xFe^{II}_yFe^{III}_zO_{4-\delta}$ were determined from the four equations

$$x + y + z = 3 \quad [1]$$

$$x/(y + z) = M_{Ni} \quad [2]$$

$$y/(y + z) = M_{Fe(II)} \quad [3]$$

$$2x + 2y + 3z = 2(4 - \delta) \text{ (electric charge balance).} \quad [4]$$

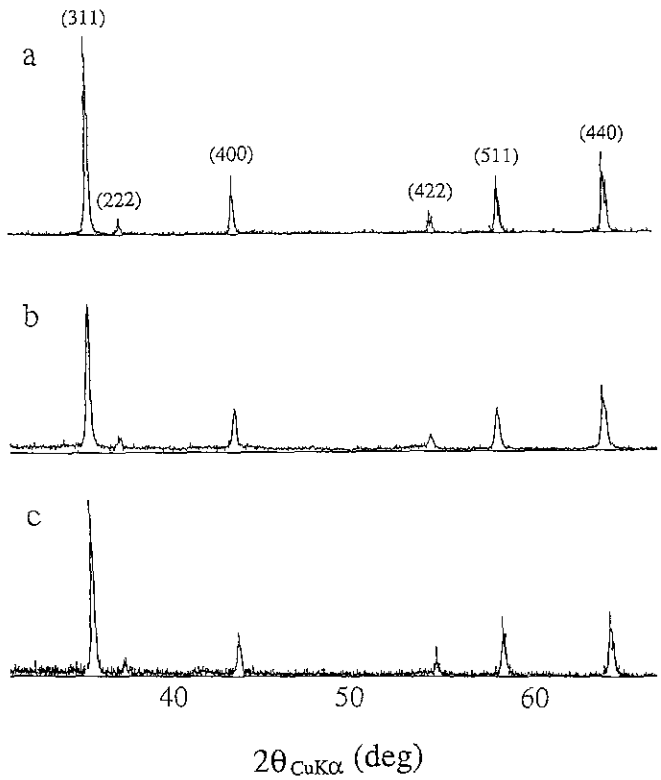

FIG. 2. XRD patterns of Ni(II)-bearing ferrites as prepared (a), H_2 reduced for 30 min (b), and after CO_2 decomposition at 300°C (c).

M_{Ni} and $M_{Fe(II)}$ represent mole ratios of Ni(II)/Fe_{total} and Fe(II)/Fe_{total} in the samples, which were determined by ICP spectroscopy and colorimetry with 2,2′-dipyridyl, respectively. The chemical composition of NF as prepared was estimated to be $Ni_{0.39}Fe_{2.61}O_{4.02}$, which was nearly stoichiometric (Table 1; sample a). The lattice constant, 0.8375 nm, was nearly equal to that of the stoichiometric Ni(II)-bearing ferrite, 0.8376 nm (20).

TABLE 1

Change in Chemical Composition and Lattice Constant of Ni(II)-Bearing Ferrite during H_2-Reduction and CO_2 Decomposition

Sample	H_2 reduction time (min)	Chemical composition	Oxygen deficiency (δ)	Lattice constant (nm)
a	0	$Ni_{0.39}Fe^{II}_{0.56}Fe^{III}_{2.05}O_{4.02}$	−0.02	0.8375
b	30	$Ni_{0.39}Fe^{II}_{0.93}Fe^{III}_{1.68}O_{3.84}$	0.16	0.8378
b*	30	$Ni_{0.39}Fe^{II}_{0.67}Fe^{III}_{1.94}O_{3.97}$	0.03	0.8377
c	60	$Ni_{0.39}Fe^{II}_{1.01}Fe^{III}_{1.60}O_{3.81}$	0.19	0.8381
c*	60	—	—	0.8379
Error			±0.004	±0.00002

Note. b* and c* are the samples after 60 min of CO_2 decomposition.

The spinel-type structure was retained in the H_2-reduced NFs. A typical XRD pattern of the NF reduced for 30 min (sample b) is given in Fig. 2b. No peaks assigned to α-Fe and metallic Ni were observed. The lattice constant of H_2-reduced NF increased with an increase in the H_2-reduction time (Table 1). The lattice constants of H_2-reduced NFs were larger than the stoichiometric value. This result indicates that the NF was transformed into oxygen-deficient NF (ODNF). The increase in the lattice constant results from changes in cation dimension and repulsion associated with reduction of Fe^{3+} to Fe^{2+} in the crystal lattice of the ferrite. From the chemical analysis, the oxygen deficiencies were estimated to be $\delta = 0.16$ and 0.19 in $Ni_{0.39}Fe_{2.61}O_{4-\delta}$ for NFs reduced for 30 (sample b) and 60 min (sample c), respectively (Table 1). It increased with the H_2-reduction time. The δ value of ODNF was the highest among those of other ODFs such as magnetite and Zn(II)- and Mn(II)-bearing ferrites prepared under the similar condition of H_2 reduction. The CO_2-decomposition reactivity shown in Fig. 1 increased with an increase in the δ value of ODNF.

The XRD patterns after CO_2 decomposition for 60 min revealed only spinel peaks (Fig. 2c). The oxygen deficiency of the sample b decreased from 0.16 to 0.03 after 60 min of CO_2 decomposition (Table 1). The oxygens of CO_2 were incorporated into the crystal lattice of ODNF and the metal oxide was restored to the chemical composition prior to H_2 reduction. The lattice constants of samples b and c after CO_2 decomposition decreased, approaching that of the stoichiometric NF. The decrease in the lattice constant of ODNF came from the fact that the larger cation dimension and repulsion in ODNF are dissolved by the incorporation of oxygens from CO_2.

3. *Mössbauer Study of H_2-Reduced NF in CO_2 Decomposition*

In the Mössbauer spectrum of the NF (sample a), only the magnetically split pattern appeared (Fig. 3), which is characteristic of the ferrites (24). The spectrum could be decomposed to two sextets indicated by a and b. The Mössbauer parameters are listed in Table 2. For magnetite Fe_3O_4, sextet a is due to the contribution of Fe^{3+} ions in the tetrahedral (A) sites, and sextet b is due to the contribution of paired Fe^{2+} and Fe^{3+} in the octahedral (B) sites, forming $Fe^{2.5+}$ in the spinel-type structure (25). The isomer shifts of the sextets a and b for magnetite are 0.28 and 0.67 mm s^{-1}, respectively (26). The isomer shifts of a and b observed for the NF were close to those for magnetite. The area ratio of sextet a to sextet b (I_a/I_b) of the NF was larger than that of magnetite (I_a/I_b = 0.5), indicating that Ni^{2+} ions occupy the B sites by replacing Fe^{2+} ions in B sites of magnetite; it is well known that Ni^{2+} ions are preferentially located at the B site (27). If one assumes that the Ni(II)-bearing ferrite

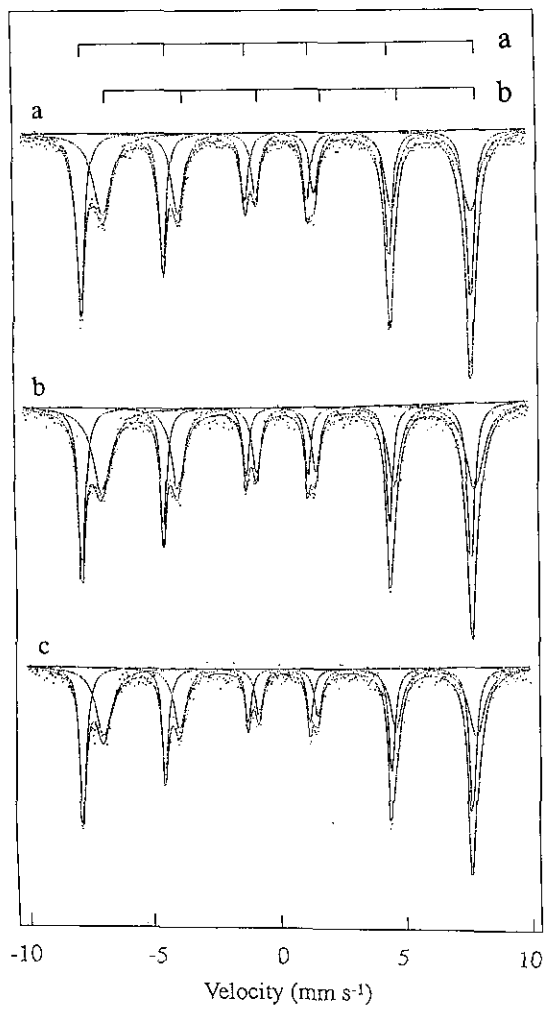

FIG. 3. Mössbauer spectra of Ni(II)-bearing ferrites as prepared (a), H_2 reduced for 30 min (b), and after CO_2 decomposition at 300°C (c).

is a "reverse spinel," the area ratio of sextet a and b (I_a/I_b) for the as-prepared material would be expected to be 0.62 ($[Fe^{3+}_{1.00}]_A[Ni^{2+}_{0.39}Fe_{1.61}]_BO_4$). The observed value, however, was 0.96. On this assumption, the mixed valence of $Fe_{1.61}$ in the B site is estimated to be 2.62, which is higher than that for magnetite, 2.5. However, the observed isomer sift of sextet b (0.66 mm/s) was nearly equal to that for magnetite (0.67 mm/s). These results imply that there is Fe^{3+}, which is not in the mixed valence state, in the B site and this Fe^{3+} in the B site contributes to the sextet a. The formation of such Fe^{3+} in B sites is reported in ferrite solid solutions such as Fe_3O_4-γ-Fe_2O_3. For the Fe_3O_4-γ-Fe_2O_3 system, sextet a is due to the contribution of Fe^{3+} in both the A and B sites, and sextet b is due to the contribution of paired Fe^{2+} and Fe^{3+} in the B sites, forming $Fe^{2.5+}$ (28). Assuming that the Fe^{3+} is present in the B site of the as-prepared Ni(II)-bearing ferrite, contributing to the sextet a, the cation distribution could be estimated from the observed I_a/I_b of 0.96 to be $[Fe^{3+}_{1.00}]_A[Ni^{2+}_{0.39}Fe^{3+}_{0.28}Fe_{1.33}]_BO_4$. The mixed valence of $Fe_{1.33}$ in the B site is 2.54, which is almost the same as that of magnetite. This assumption is supported by the fact that the observed isomer sift of sextet b was nearly equal to that for magnetite.

The Mössbauer spectrum of the ODNF prepared by 30 min of H_2 reduction (sample b) was similar to that of the NF (Fig. 3b). The absorption peaks indicating the α-Fe phase were not observed. The ODNF after CO_2 decomposition also gave only the magnetically split pattern decomposed to two sextets (Fig. 3c). The I_a/I_b of ODNF (sample b) before CO_2 decomposition was significantly larger than that of the NF (sample a), indicating that the arrangement of iron ions among A and B sites in NF was changed by H_2 reduction. The decrease in I_a/I_b would arise from the fact that some of the iron ions in A sites migrate to B sites in the spinel-type structure. It is considered that the excess iron ions formed by H_2 reduction occupy the interstices of B sites in ODNF at 300°C as mentioned later. The I_a/I_b of ODNF increased after CO_2 decomposition approaching that of the NF. The arrangement of iron ions will be restored to that prior to H_2 reduction by incorporating oxygen from CO_2.

The magnetic hyperfine field did not change throughout the H_2 reduction and subsequent CO_2 decomposition, indicating the magnetic environment of iron ions in the A and B sites of ODNF is not so different from that of the NF.

TABLE 2
Change in Mössbauer Parameters of Ni(II)-Bearing Ferrite by H_2 Reduction and CO_2 Decomposition

Material	I_a/I_b	Isomer shift (mm s^{-1})		Quadrupole splitting (mm s^{-1})		Magnetic hyperfine field (10^6 A m^{-1})	
		Site A	Site B	Site A	Site B	Site A	Site B
As prepared	0.963	0.29	0.66	−0.02	0.08	−39.7	−36.9
30 min reduction	0.748	0.28	0.65	−0.01	0.08	−38.9	−37.3
After CO_2 decomposition	0.903	0.28	0.66	−0.02	0.10	−38.9	−37.2
Error	±0.02	±0.01		±0.01		±0.4	

Neither the isomer shift nor quadrupole splitting were changed by H_2 reduction and by CO_2 decomposition.

From these results, the cation migration in the NF during H_2 reduction and subsequent CO_2 decomposition is considered to proceed as follows. (i) The lattice oxygens on the surface of NF are removed by H_2 and the Fe^{3+} ion is reduced to Fe^{2+} on the surface. (ii) The excess cations formed by the H_2 reduction on the surface migrate to the inside of the solid phase. The Fe^{2+} ion is known to preferentially occupy the B site (27): magnetite is a inverse spinel. The excess Fe^{2+} ion will be situated in interstices of B sites in the bulk inside due to its B site preference. (iii) The excess cations migrate from the inside to the surface during the CO_2 decomposition. (iv) On the surface, the Fe^{2+} ion is oxidized to Fe^{3+} to release the electron to CO_2. The excess cations and O^{2-} ions from CO_2 make the spinel structure on the surface. The arrangement of the cations in the spinel-type structure is restored to that prior to H_2 reduction. These processes can be written by the equations

$$Fe^{3+} + 1/2O^{2-}_{lat} + 1/2H_2 \rightarrow Fe^{2+}_{int(B)} + 1/2H_2O \quad [5]$$

$$Fe^{2+}_{int(B)} + 1/4CO_2 \rightarrow Fe^{3+} + 1/2O^{2-}_{lat} + 1/4C. \quad [6]$$

Fe^{3+} and $Fe^{2+}_{int(B)}$ represent the ferric ion in the normal lattice position and the ferrous ion in the interstitial position of the B site. O^{2-}_{lat} indicates the lattice oxygen ion. Ni^{2+} ions in the ferrite may migrate during H_2 reduction and CO_2 decomposition. Excess Ni^{2+} ion formed by the H_2 reduction of NF will probably occupy the interstices of B sites due to its B site preference. However, the Ni^{2+} migration has not been examined because Ni^{2+} could not be detected by the Mössbauer analysis in the present work.

CONCLUSIONS

The oxygen-deficient Ni(II)-bearing ferrite was formed by H_2 reduction at 300°C. The lattice constant of ODNF was larger than that of the stoichiometric Ni(II)-bearing ferrite. The increase in the lattice constant will come from changes in the cation dimension and repulsion associated with the reduction of Fe^{3+} to Fe^{2+} in the crystal lattice of the ferrite. The oxygen deficiency of ODNF increased with an increase in the H_2 reduction time. The maximum value was found to be $\delta = 0.19$ at the reduction time = 60 min under the present experimental condition. The δ value of ODNF was the highest among those of other ODFs such as magnetite and Zn(II)- and Mn(II)-bearing ferrites prepared under the similar condition of H_2 reduction. The reactivity of ODNF for decomposition of CO_2 to carbon at 300°C increased with a higher δ value. The oxygen deficiency and lattice constant of ODNF decreased after CO_2 decomposition, being restored to the stoichiometric values.

From the Mössbauer spectra, it was found that the area ratio of sextet a to b of ODNF drastically decreased in comparison to that of the NF. This would be due to the migration of the iron ions from A sites to B sites in the spinel-type structure. It is considered that excess iron ions formed by H_2 reduction are situated in the interstices of the B sites. The I_a/I_b of ODNF increased after CO_2 decomposition, approaching that of the NF. This suggests that excess iron ions in the interstices of the B sites migrate to A sites in the spinel structure of ODNF by incorporating the oxygens from CO_2. The arrangement of iron ions is considered to be restored to that of stoichiometric NF during CO_2 decomposition.

ACKNOWLEDGMENTS

The present work was partially supported by Grant-in-Aid for Science Research No. 06403030 and 06558067 from the Ministry of Education, Science, and Culture. One of the authors (T.K.) is grateful for grants from Fellowships of the Japan Society for the Promotion of Science for Japanese Junior Scientists.

REFERENCES

1. E. J. W. Verwey and P. W. Haayman, *Physica* **8,** 979 (1941).
2. H. Annersten and S. S. Hafner, *Z. Kristallogr.* **137,** 321 (1973).
3. P. Mollard, A. Collomb, J. Devenyi, A. Rousset, and J. Pâris, *I.E.E.E. Trans. Magn.* **11,** 894 (1975).
4. B. Guillot, A. Pousset, and G. Dupre, *J. Solid State Chem.* **25,** 263 (1978).
5. T. Kodama, *J. Mater. Chem.* **2,** 525 (1992).
6. Y. Tamaura and M. Tabata, *Nature (London)* **346,** 255 (1990).
7. Y. Tamaura and K. Nishizawa, *Energy Convers. Manage.* **33,** 573 (1992).
8. M. Tabata, Y. Nishida, T. Kodama, K. Mimori, T. Yoshida, and Y. Tamaura, *J. Mater. Sci.* **28,** 971 (1993).
9. M. Tabata, K. Akanuma, K. Nishizawa, K. Mimori, T. Yoshida, M. Tsuji, and Y. Tamaura, *J. Mater. Sci.* **28,** 6753 (1993).
10. M. Tabata, K. Akanuma, T. Togawa, M. Tsuji, and Y. Tamaura, *J. Chem. Soc. Faraday Trans.* **90,** 1171 (1994).
11. K. Nishizawa, T. Kodama, M. Tabata, T. Yoshida, M. Tsuji, and Y. Tamaura, *J. Chem. Soc. Faraday Trans.* **88,** 2772 (1992).
12. T. Kodama, M. Tabata, K. Tominaga, T. Yoshida, and Y. Tamaura, *J. Mater. Sci.* **28,** 547 (1993).
13. M. Tabata, H. Kato, T. Kodama, T. Yoshida, M. Tsuji, and Y. Tamaura, *J. Mater. Sci.* **29,** 999 (1994).
14. T. Yoshida, K. Nishizawa, M. Tabata, H. Abe, T. Kodama, M. Tsuji, and Y. Tamaura, *J. Mater. Sci.* **28,** 1220 (1993).
15. K. Nishizawa, H. Kato, K. Mimori, T. Yoshida, N. Hasegawa, M. Tsuji, and Y. Tamaura, *J. Mater. Sci.* **29,** 768 (1994).
16. M. Tsuji, K. Nishizawa, T. Yoshida, and Y. Tamaura, *J. Mater. Sci.* **29,** 5481 (1994).
17. T. Kodama, H. Kato, S. G. Chang, N. Hasegawa, M. Tsuji, and Y. Tamaura, *J. Mater. Res.* **9,** 462 (1994).
18. H. Kato, T. Kodama, M. Tsuji, Y. Tamaura, and S. G. Chang, *J. Mater. Sci.* **29,** 5689 (1994).
19. T. Katsura, Y. Tamaura, and G. S. Chyo, *Bull. Chem. Soc. Jpn.* **52,** 96 (1979).

20. H. Kato, M. Tabata, M. Tsuji, and Y. Tamaura, *in* "Materials and Processes for Environmental Protection" (K. E. Voss, L. M. Quick, P. N. Gadgil, and C. L. G. Adkins, Eds.), Vol. 344, p. 163. Materials Research Society, Pittsburgh, 1994.
21. T. Yamamoto, T. Kodama, T. Sano, M. Tsuji, and Y. Tamaura, submitted for publication.
22. I. Iwasaki, T. Katsura, T. Ozawa, M. Yoshida, M. Mishima, H. Haramura, and B. Iwasaki, *Bull. Volcanol. Soc. Jpn. Ser. II* **5,** 9 (1960).
23. J. B. Nelson and D. P. Riley, *Proc. Phys. Soc.* **57,** 160 (1945).
24. J. W. Linnett and M. M. Rahman, *J. Phys. Chem. Solids* **33,** 1465 (1972).
25. J. M. Daniels and A. Rosencwaig, *J. Phys. Chem. Solids* **30,** 1561 (1969).
26. M. Robbins, G. K. Wertheim, R. C. Sherwood, and D. N. E. Buchanan, *J. Phys. Chem. Solids* **32,** 717 (1971).
27. J. Smit and H. P. J. Wijn, "Ferrites," p. 140. Cleaver–Hume, London, 1959.
28. H. Franke and M. Rosenberg, *J. Magn. Magn. Mater.* **9,** 74 (1979).